




# Immune-related lncRNA pairs as novel signature to predict prognosis and immune landscape in melanoma patients

Zhehong Li, MD<sup>a</sup> , Junqiang Wei, MD<sup>a</sup> , Honghong Zheng, MD<sup>b</sup> , Xintian Gan, MD<sup>a</sup>, Mingze Song, MD<sup>a</sup>, Yafang Zhang, MD<sup>a</sup>, Yu Jin, PhD<sup>a,\*</sup>

## Abstract

To investigate immune-related long non-coding RNA (lncRNA) signatures for predicting survival and the immune landscape in melanoma patients.

We retrieved gene expression files from The Cancer Genome Atlas and the Genotype-Tissue Expression database and extracted all the long non-coding RNAs from the original data. Then, we selected immune-related long non-coding RNAs (lncRNAs) using co-expression networks and screened differentially expressed lncRNAs (DElncRNAs) to form pairs. We also performed univariate analysis and Least absolute shrinkage and selection operator (LASSO) penalized regression analysis to identify prognostic DElncRNA pairs, constructed receiver operating characteristic curves, compared the areas under the curves, and calculated the optimal cut-off point to divide patients into high-risk and low-risk groups. Finally, we performed multivariate Cox regression analysis, Kaplan–Meier (K–M) survival analysis, clinical correlation analysis, and investigated correlations with tumor-infiltrating immune cells, chemotherapeutic effectiveness, and immunogene biomarkers.

A total of 297 DElncRNAs were identified, of which 16 DElncRNA pairs were associated with prognosis in melanoma. After grouping patients by the optimal cut-off value, we could better distinguish melanoma patients with different survival outcomes, clinical characteristics, tumor immune status changes, chemotherapeutic drug sensitivity, and specific immunogene biomarkers.

The DElncRNA pairs showed potential as novel biomarkers to predict the prognosis of melanoma patients. Furthermore, these DElncRNA pairs could be used to evaluate treatment efficacy in the future.

**Abbreviations:** AUC = area under the curve, CTLA-4 = cytotoxic T lymphocyte associate protein-4, DElncRNAs = differentially expressed immune-related long non-coding RNAs, ICI = immune checkpoint inhibitor, lncRNAs = immune-related long non-coding RNAs, K–M = Kaplan–Meier, LASSO = least absolute shrinkage and selection operator, lncRNAs = long non-coding RNAs, mRNA = messenger RNA, PD-1 = programmed cell death protein 1, PD-L1 = programmed cell death protein ligand-1, ROC = receiver operating characteristic, TCGA = the cancer genome atlas.

**Keywords:** immune, long non-coding RNAs, melanoma, prognosis, treatment

Editor: Soroush Niknamian.

ZL and JW contributed equally to this work.

Because we use public and anonymous data, according to the ethics guidelines, neither informed consent nor approval of the ethics committee is required.

The authors have no funding and conflicts of interests to disclose.

Supplemental Digital Content is available for this article.

The datasets generated during and/or analyzed during the current study are available from the corresponding author on reasonable request.

<sup>a</sup> Traumatology and Orthopedics, Affiliated Hospital of Chengde Medical College, Chengde, Hebei, China, <sup>b</sup> Department of General Surgery, Affiliated Hospital of Chengde Medical College, Chengde, Hebei, China.

\* Correspondence: Yu Jin, Traumatology and Orthopedics, Affiliated Hospital of Chengde Medical College, Chengde, Hebei, China (e-mail: cdyxyjy@126.com).

Copyright © 2022 the Author(s). Published by Wolters Kluwer Health, Inc. This is an open access article distributed under the terms of the Creative Commons Attribution-Non Commercial License 4.0 (CCBY-NC), where it is permissible to download, share, remix, transform, and buildup the work provided it is properly cited. The work cannot be used commercially without permission from the journal.

How to cite this article: Li Z, Wei J, Zheng H, Gan X, Song M, Zhang Y, Jin Y. Immune-related lncRNA pairs as novel signature to predict prognosis and immune landscape in melanoma patients. *Medicine* 2022;101:1(e28531).

Received: 16 September 2021 / Received in final form: 17 December 2021 / Accepted: 21 December 2021

<http://dx.doi.org/10.1097/MD.00000000000028531>

## 1. Introduction

Malignant melanoma is the most aggressive skin cancer and has a high mortality rate. There were approximately 100,000 newly diagnosed melanoma cases and more than 7000 melanoma deaths in the United States in 2019,<sup>[1]</sup> and the incidence of melanoma is projected to increase globally. According to the GLOBOCAN data, there were 287,723 new melanoma cases and 60,712 deaths worldwide in 2018,<sup>[2]</sup> compared with 232,130 new cases and 55,488 deaths in 2012.<sup>[3]</sup> Melanoma more commonly affects Caucasian white populations than those with pigmented skin such as Hispanics, Africans, and Asians: an estimated 21.2 per 100,000 population were newly diagnosed with melanoma in Western countries between 2006 and 2010, compared with less than 1 per 100,000 in East Asian countries including China, Japan, South Korea, and Singapore.<sup>[4]</sup> More than half of melanoma patients are stage I at the time of diagnosis and have a 5-year survival rate of 60% to 70%; however, in advanced-stage patients, the 5-year survival rate decreases to 19%<sup>[5]</sup> and the median overall survival is 0 to 9 months.<sup>[6]</sup> Owing to the poor prognosis of patients with metastatic malignant melanoma, current efforts tend to focus on improving early diagnosis.

In the past decade, the prognosis of advanced melanoma patients has been greatly improved by the use of immune

checkpoint inhibitors (ICIs), including cytotoxic T lymphocyte associate protein-4 (CTLA-4) inhibitor and programmed cell death protein 1 (PD-1)/programmed cell death ligand-1 (PD-L1) inhibitors. However, 40% of patients show limited or no response to immunotherapy.<sup>[7]</sup> Therefore, the development of immune-related biomarkers is of great significance for evaluating the prognosis of patients and their response to treatment with ICIs. Many studies have assessed the relationship between the prognosis of melanoma patients and levels of various non-coding RNAs.<sup>[8–10]</sup> However, there is a lack of non-coding RNAs that are suitable as biomarkers to evaluate the effects of immunotherapy in melanoma patients. Inspired by the research of Lv et al,<sup>[11]</sup> we aimed to establish a signature combining long non-coding RNA (lncRNA) pairs to assess the prognosis of melanoma patients.

Long non-coding RNAs (lncRNAs) are transcripts that are more than 200 nucleotides in length and have no protein-coding potential. They can regulate chromatin modification, transcription, and post-transcriptional processing at different levels.<sup>[12,13]</sup> Furthermore, lncRNAs can affect the proliferation and apoptosis of tumor cells, promote their migration and invasion, and mediate the development of drug resistance, as well as regulating the formation of tumor blood vessels.<sup>[14–16]</sup> Many studies have shown that lncRNAs are related to the activation or suppression of various immune cells and directly or indirectly involved in tumor immune regulation.<sup>[17,18]</sup> Wu et al identified a signature consisting of 8 immune-related lncRNAs (irlncRNAs) that could predict prognosis and immunotherapy response in bladder cancer.<sup>[19]</sup> Such irlncRNAs are of great value in evaluating tumor characteristics, prognosis, and treatment.<sup>[11,20]</sup> Compared to multiple gene combinations, two-gene combination strategy can provide relative expression within a sample, leading to more robust and accurate speculation.<sup>[11,21,22]</sup> At the same time, the relative expression of gene pairs takes into account all possible combinations.<sup>[23]</sup> Therefore, developing new irlncRNAs to treat melanoma is of great significance and could improve the quality of life of patients. To the best of our knowledge, there have been few attempts to predict prognosis and the immune landscape in cancer using a two-gene combination strategy composed of irlncRNAs. Therefore, we aimed to construct irlncRNA-pair signatures and evaluate their predictive value with respect to diagnostic effect, chemotherapeutic efficacy, and tumor immune invasion.

## 2. Materials and methods

### 2.1. Retrieval and collection of transcriptome data and identification of differentially expressed irlncRNAs

A flowchart of the process is shown in Figure 1. RNA sequencing data for 558 normal skin tissue samples (1 from The Cancer Genome Atlas [TCGA] and 557 from the Genotype-Tissue Expression databases) and 471 melanoma tissues (from TCGA) were obtained from the University of California Santa Cruz Xena browser (<https://xenabrowser.net/>). The fragments per kilobase million values of all samples were normalized to log<sub>2</sub> (Fragments Per Kilobase Million + 1). Merged data from different databases in the genetic Ensembl format were annotated using gene transfer format files (<http://asia.ensembl.org>). Messenger RNAs (mRNAs) and lncRNAs were distinguished according to the corresponding naming rules in the Gene Transfer Format files. Known immune-related genes were downloaded from IMMPORT (<https://www.immport.org/>), and co-expression analysis was performed between lncRNAs and these genes. The selection criteria for irlncRNAs

were: correlation coefficient greater than 0.4 and *P* value less than .001. irlncRNAs were confirmed for subsequent analysis. Differentially expressed irlncRNAs (DEirlncRNAs) in melanoma were identified using the “limma” package in the R software. The screening criteria for DEirlncRNAs were: log (fold change) greater than 1.0 and false discovery rate less than 0.05. Heat maps and volcano plots were used to visualize the results.

### 2.2. Establishment of two-gene combination strategy and risk assessment model

All possible pairs of DEirlncRNAs (denoted lncRNA-A and lncRNA-B, respectively) were identified and assessed based on the following definitions: (I) if the ratio of lncRNA-A expression to lncRNA-B expression was greater than 1, the pair was defined as lncRNA-A|lncRNA-B=1; (II) if the ratio of lncRNA-A expression to lncRNA-B expression was less than 1, the pair was defined as lncRNA-A|lncRNA-B=0; (III) for a given pair, if lncRNA-A|lncRNA-B=1 in more than 80% of all patients, the pair was considered invalid; and (IV) if lncRNA-A|lncRNA-B=0 in more than 80% of all patients, the pair was also considered invalid.<sup>[21]</sup> Valid DEirlncRNA pairs were identified by applying these definitions and used to construct a matrix with each entry corresponding to the value of the respective lncRNA-A|lncRNA-B. Combining clinical survival status and survival time data from TCGA, prognostic DEirlncRNA pairs were obtained by univariate Cox regression analysis and least absolute shrinkage and selection operator (LASSO) regression analysis.<sup>[24]</sup> Independent prognostic DEirlncRNA pairs were identified by multivariate Cox regression analysis. Then, receiver operating characteristic (ROC) curves were plotted based on the prognostic related genes' characteristics, and the corresponding area under the curve (AUC) values were determined. Risk scores were calculated for each patient using the following formula:

$$\text{Risk score} = \sum_i^n \text{coef}(\text{DEirlncRNA pairs}_i) \times \text{expr}(\text{DEirlncRNA pairs}_i),$$

where coef (DEirlncRNA pairs<sub>*i*</sub>) and expr (DEirlncRNA pairs<sub>*i*</sub>) represent the survival correlation coefficient of DEirlncRNA pair and the DEirlncRNA pair matrix of patients, respectively.

Using an optimal cut-off point based on the risk score, we reclassified the melanoma cohort into a high-risk group and a low-risk group for further validation.

### 2.3. Clinical evaluation by risk assessment model

Kaplan–Meier (K–M) analysis was used to describe the survival of melanoma patients. We visualized the relationship between melanoma risk and clinicopathological characteristics using a heat map. Univariate and multivariate Cox regression analyses were used to assess patients' clinicopathological features (including age, sex, clinical stage, T stage, N stage, and M stage) and risk scores to identify prognostic factors. ROC curves were drawn for comparison.

### 2.4. Analyses of tumor immune cell infiltration and expression of ICI-related immunosuppressive molecules and kinase inhibitors

A detailed Spearman correlation analysis was conducted between tumor-infiltrating immune cells and the risk assessment model, and a

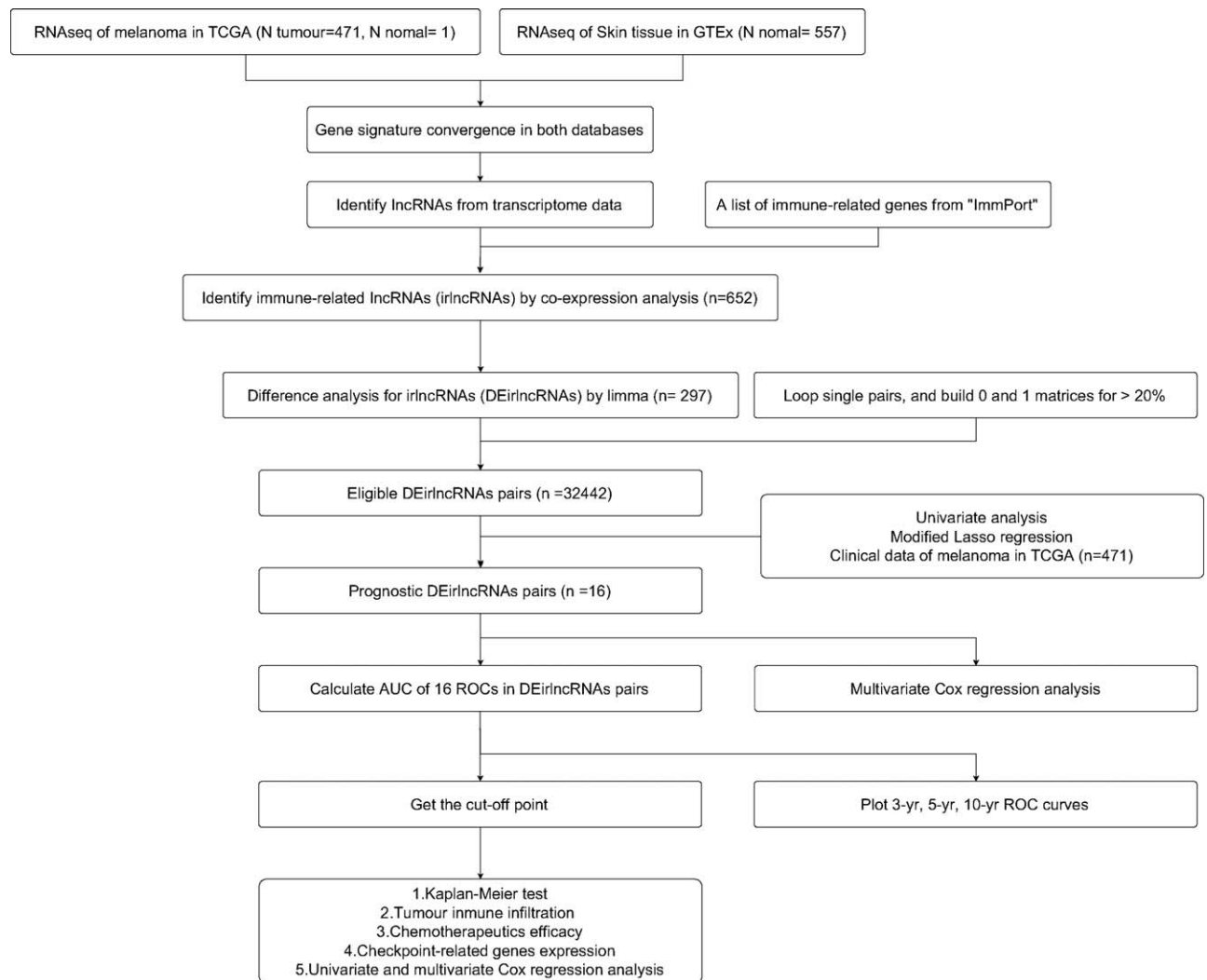


Figure 1. Flow chart of the study.

lollipop chart was constructed.<sup>[25]</sup> To investigate the relationship between risk score and tumor-infiltrating immune cells, 7 methods were used to evaluate immune infiltrating cells: TIMER,<sup>[26]</sup> CIBERSORT,<sup>[27]</sup> xCell,<sup>[28]</sup> quanTIseq,<sup>[29]</sup> MCP-counter,<sup>[30]</sup> EPIC<sup>[30]</sup> and CIBERSORT-ABS.<sup>[31]</sup> We further analyzed the relationships of the risk assessment model with ICI-related biomarkers (CTLA-4 and PD-1/PD-L1) and kinase inhibitor biomarkers (B-Raf Proto-Oncogene, KIT Proto-Oncogene, NRAS Proto-Oncogene, KRAS Proto-Oncogene, and HRAS Proto-Oncogene).

### 2.5. Correlation analysis between risk models and chemotherapy agents

The “Prophetic” R package was used to identify associations between the risk model and chemotherapy (imatinib,<sup>[32]</sup> cisplatin,<sup>[33]</sup> and paclitaxel<sup>[34]</sup>) in melanoma using the TCGA melanoma data-set.

### 2.6. Statistical analysis

All analyses were carried out by R version 4.0.3 and corresponding packages. Differences in quantitative data and normally distributed variables were compared using the *t*-test,

and differences in non-normally distributed variables were compared using the Wilcoxon rank-sum test. Differences were compared for more than 2 groups of variables using one-way analysis of variance and the Kruskal–Wallis test. Prognostic analysis was performed using the K–M survival analysis and Cox proportional hazards model.

## 3. Results

### 3.1. Identification of DElncRNAs

A total of 652 irlncRNAs were identified (more details are shown in Supplemental Digital Content, Table S1, <http://links.lww.com/MD2/A827>). These included 297 DElncRNAs, as shown in the heat map in Figure 2A, of which 245 were upregulated and 52 were downregulated (see volcano map in Fig. 2B).

### 3.2. Establishment of two-gene combination strategy and risk assessment model

A total of 32442 valid DElncRNA pairs were obtained, among which 16 independent prognostic DElncRNA pairs were identified by Cox regression analysis and LASSO regression analysis. The results of the univariate Cox regression analysis and

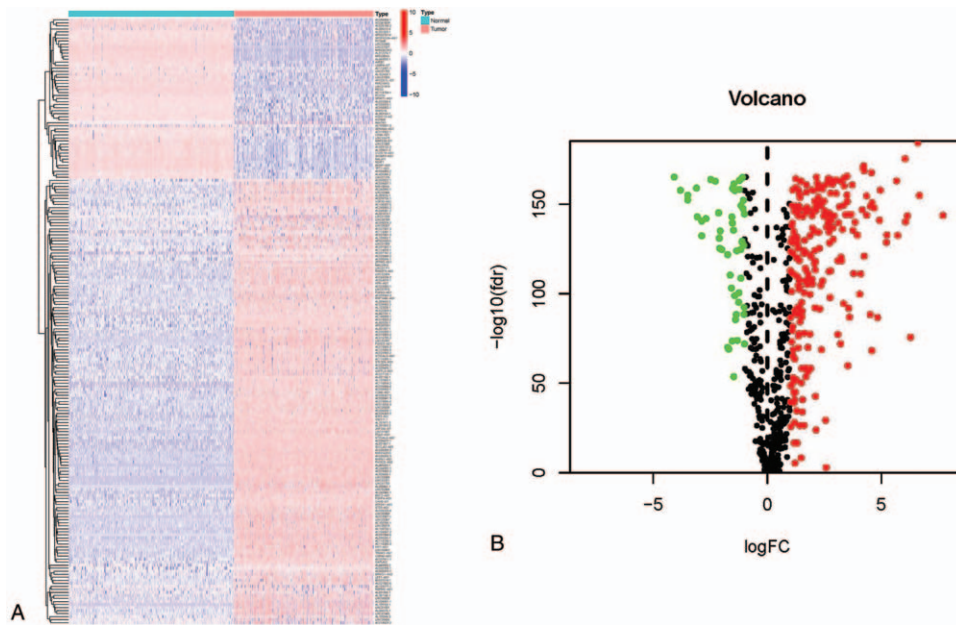


**Figure 2.** Establishment of DElncRNA pairs. (A) Heat map of immune-related lncRNAs with significant differences. (B) Volcano plot of immune-related lncRNAs; green indicates downregulated genes, and red indicates upregulated genes.

LASSO regression analysis are shown in Figure 3A and 3B-C, respectively. The results of the multivariate Cox regression analysis are shown in Figure 3D. The 16 independent prognostic DElncRNA pairs were as follows: AC087741.2|AC103591.3, AC087741.2|MIR3142HG, AC087741.2|GSEC, ADIRF-AS1|SPINT1-AS1, AC004847.1|LINC02446, AC027130.1|AL034376.1, AC022034.1|FOXP4-AS1, USP30-AS1|HOTAIR, USP30-AS1|AC055854.1, USP30-AS1|SERPINB9P1, USP30-AS1|AL049555.1, USP30-AS1|AP000759.1, AP003392.4|ATP2B1-AS1, AP003392.4|AC009495.2, AP003392.4|RNF144A-AS1, and AP003392.4|LINC01819. The ROC curves for these 16 DElncRNA pairs were shown in Figure 4A. The AUC value and the optimal cut-off point were 0.795 and 2.050, respectively. ROC curves for 3-, 5-, and 10-year survival predicted by the risk assessment model are shown in Figure 4B; the 3-, 5-, and 10-year AUC values were 0.744, 0.786, and 0.794, respectively. A comparison of ROC curves with clinical features is shown in Figure 4C.

### 3.3. Clinical evaluation by risk assessment model

The risk score and survival outcome from TCGA for each case are shown in Figure 5A-B. K-M analysis showed that patients in the high-risk group had a shorter survival time than those in the low-risk group ( $P < .001$ ; Fig. 5C). The strip chart (Fig. 6A) and scatter plot obtained by Chi-Squared independence test showed that age (Fig. 6B), T stage (Fig. 6C), and N stage (Fig. 6D) were associated with risk score. However, sex, M stage, and clinical stage were not correlated with risk score ( $P > .05$ ; Supplemental Digital Content, Figure S1, <http://links.lww.com/MD2/A821>).

### 3.4. Analyses of tumor immune cell infiltration and expression of ICI-related immunosuppressive molecules and kinase inhibitors

Patients in the high-risk group were more positively correlated with the infiltration of certain immune cells, including resting natural

killer cells (CIBERSORT-ABS) and natural killer T cells (xCell). By contrast, they were negatively associated with CD4+memory T cells (xCell) and CD8+central memory T cells (xCell), etc. Detailed Spearman correlation analysis was conducted; the resulting lollipop graph is shown in Figure 7. More results of the Spearman analysis of tumor-infiltrating immune cells using different software are shown in Supplemental Digital Content, Figures S2–S6, <http://links.lww.com/MD2/A822>, <http://links.lww.com/MD2/A823>, <http://links.lww.com/MD2/A824>, <http://links.lww.com/MD2/A825>, <http://links.lww.com/MD2/A826>. Comparison of the risk model with ICI-related biomarkers showed that the high-risk group was positively correlated with low expression of CTLA-4 ( $P < .001$ ; Fig. 8A) and PD-1 ( $P < .001$ ; Fig. 8B). Further comparison of the risk model with kinase inhibitor biomarkers showed that the high-risk group was positively correlated with low expression of B-Raf Proto-Oncogene ( $P < .001$ ; Fig. 8C), NRAS Proto-Oncogene ( $P < .05$ ; Fig. 8D), and KRAS Proto-Oncogene ( $P < .05$ ; Fig. 8E). The high-risk group was positively correlated with high expression of KIT Proto-Oncogene ( $P < .05$ ; Fig. 8F) and HRAS Proto-Oncogene ( $P < .01$ ; Fig. 8G).

### 3.5. Estimation of the correlation between the risk model and clinical treatment

Comparing the high-risk group and the low-risk group, we found that in the high-risk group, high half-maximal inhibitory concentration values were observed for certain chemotherapy regimens, including cisplatin ( $P = 1.5e^{-07}$ ; Fig. 8H); however, there were low half-maximal inhibitory concentration values for other drugs including imatinib ( $P = 4.4e^{-06}$ ; Fig. 8I) and paclitaxel ( $P = .037$ ; Fig. 8J).

## 4. Discussion

Malignant melanoma is the most aggressive skin cancer and has a high mortality rate.<sup>[2,35,36]</sup> The prognosis of advanced melanoma

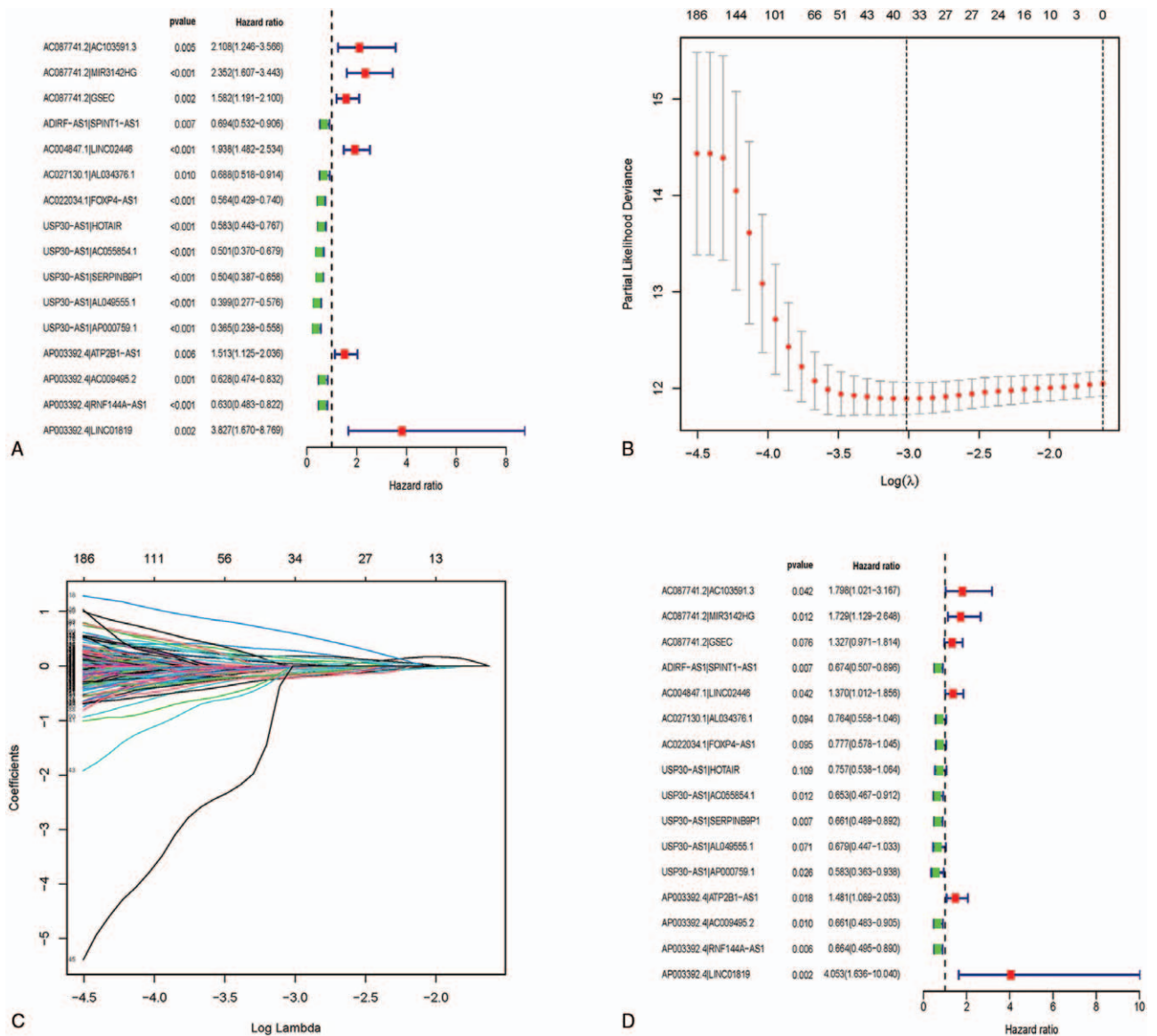


**Figure 3.** Establishment of a risk assessment model using DEirIncRNAs. (A) Univariate analysis of DEirIncRNA pairs. (B, C). LASSO was used to screen overall survival related lncRNAs. (D) Multivariate Cox regression analysis of DEirIncRNA pairs.

has improved greatly owing to the development of ICI therapy; however, in 60% of patients, ICIs have limited efficacy or elicit no response.<sup>[7,37]</sup> Therefore, it is important to explore potential therapeutic targets and prognostic indicators in melanoma. For these reasons, research has increasingly focused on lncRNAs, especially irlncRNAs.<sup>[38,39]</sup> Previous studies have confirmed that lncRNAs have crucial roles in regulating the occurrence and development of various tumor types.<sup>[40-42]</sup> In the present study, we aimed to construct a novel signature composed of DEirIncRNA pairs to evaluate the prognosis of melanoma patients.

Many studies have assessed the prognosis of melanoma patients by analyzing coding or non-coding RNAs,<sup>[8-10]</sup> usually based on quantitative analysis of RNA transcription levels. Guo et al analyzed the expression levels of 16 lncRNAs and constructed a signature to predict prognosis of melanoma patients.<sup>[43]</sup> Zhang et al constructed a lncRNA-mRNA regulation module containing 6 lncRNAs and 4 target mRNAs, again

for prognostic assessment in melanoma patients.<sup>[44]</sup> However, a problem with such approaches is that the low frequency of a single differentially expressed gene may lead to a high rate of missed diagnoses.<sup>[11]</sup> Inspired the research of Lv et al<sup>[11]</sup> we established a prognostic signature for melanoma based on combined DEirIncRNA pairs. This process does not require measurement of specific transcriptional expression levels of RNAs; instead, a matrix with entries 0 or 1 is constructed based on comparisons of the expression of DEirIncRNAs. In contrast to previous research, our study aimed to identify DEirIncRNAs and establish the most critical DEirIncRNA pairs. Therefore, we only needed to detect high- or low-expression pairs and did not need to examine the specific expression value of each lncRNA. This novel model has excellent clinical practicality; it not only distinguishes high-risk clinical cases but can also reduce the error-correction work required, making it suitable for use by researchers or clinicians from different backgrounds.

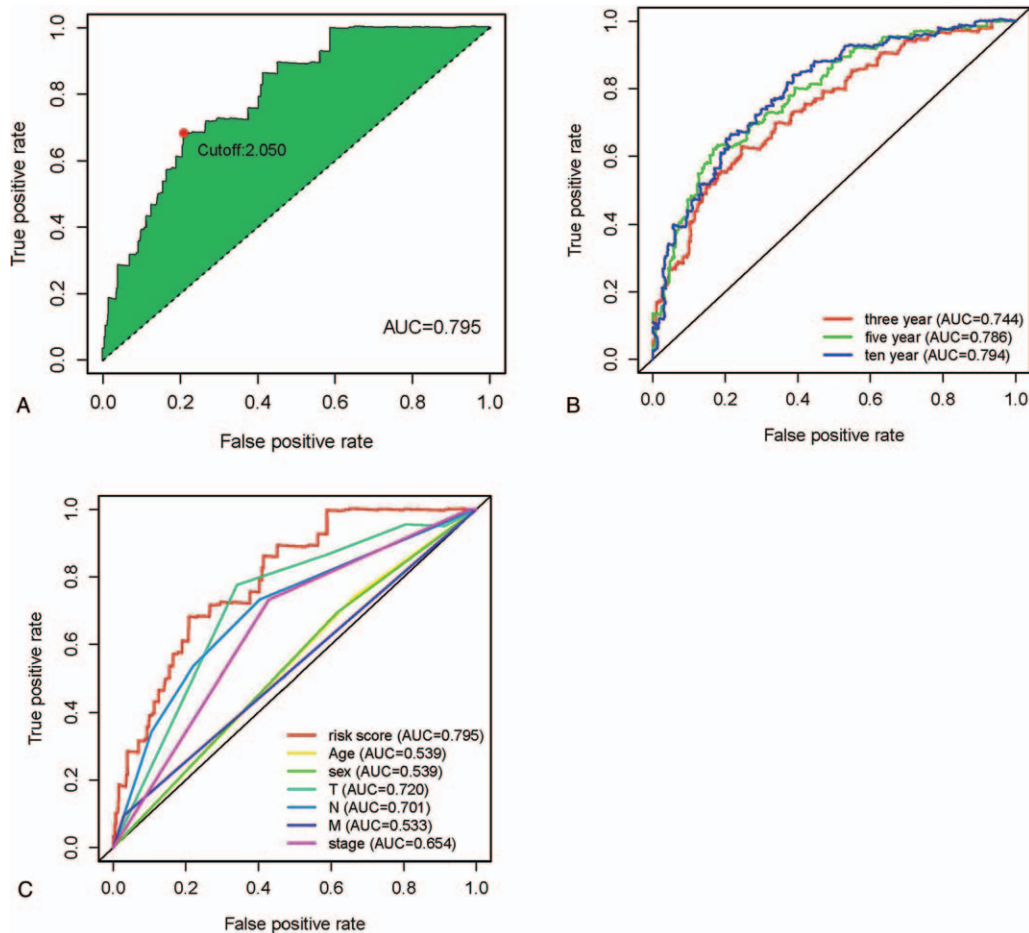


**Figure 4.** Establishment of a risk assessment model using DElncRNA pairs. (A) ROC curve for 16 DElncRNA pairs and optimal cut-off point. (B) 3-, 5-, and 10-year survival ROC curve for risk assessment model. (C) Comparison of ROC curves with other clinical features.

With the development of anti-PD-1 and anti-CTLA-4 agents, there has been constant innovation in the treatment of melanoma.<sup>[45,46]</sup> Our results showed that PD-1 and CTLA-4 expression was downregulated in the high-risk group. It should be noted that PD-1 and PD-L1 blockade is only effective in patients with high PD-1 or PD-L1 expression.<sup>[47]</sup> Topalian et al found that 17 PD-L1-negative patients had no blocking reaction when treated with a PD-1 inhibitor, whereas 9 of 25 PD-L1-positive patients reacted to ICI treatment ( $P < .05$ ).<sup>[48]</sup> Shang et al found that low expression of PD-1 in uveal melanoma was an indicator of less infiltration of immune cells.<sup>[49]</sup> Therefore, we speculated that the low expression of PD-1 in the high-risk-score group might be accompanied by less infiltration of immune cells combined with PD-1 inhibitor resistance, resulting in a shorter survival time. Higashikawa et al showed that high expression of CTLA-4 was associated with tumor-infiltrating T cells.<sup>[50]</sup> Ciszak et al conjectured that CTLA-4 inhibitors induced survival-promoting signals in tumor cells of patients with high CTLA-4 expression.<sup>[51]</sup> Therefore, the survival time of patients in the low-risk group with high expression of CTLA-4 was longer than that of patients in the high-risk group. Melanoma is often accompanied by an abnormal Mitogen-Activated Protein Kinase pathway; key molecules of this pathway include RAS and RAF.<sup>[52,53]</sup> Therefore, in addition to ICI-related biomarkers, we compared

the expression of key biomarkers of kinase inhibitors in the high- and low-risk groups.

Different types of tumor-infiltrating immune cells can upregulate or downregulate melanoma immunity in the microenvironment.<sup>[54]</sup> By comparing the correlations of immune cells in the high- and low-risk groups, we found that immune cell infiltration was lower in the high-risk group than in the low-risk group. Immune cells are a major component of the tumor microenvironment and are closely related to tumor cell proliferation, treatment response, and prognosis.<sup>[55,56]</sup> Previous studies have shown that a higher degree of immune cell infiltration in melanoma is associated with a more significant response to ICIs.<sup>[57,58]</sup> Therefore, based on the combined results of the survival analysis and measurement of immune cell infiltration and expression of ICI markers in the high- and low-risk groups, we speculated that melanoma patients with low levels of immune cell infiltration and ICI marker expression would have low sensitivity to immune-related therapies, resulting in poor prognosis.

When we compared the patients' clinicopathological characteristics with the results of the risk model, we found that older patients tended to have higher risk scores ( $P = .049$ , Fig. 6B). Patients with stage T4 melanoma also had higher risk scores than those in stages T0–T3 (Fig. 6C). Balch et al reached a similar

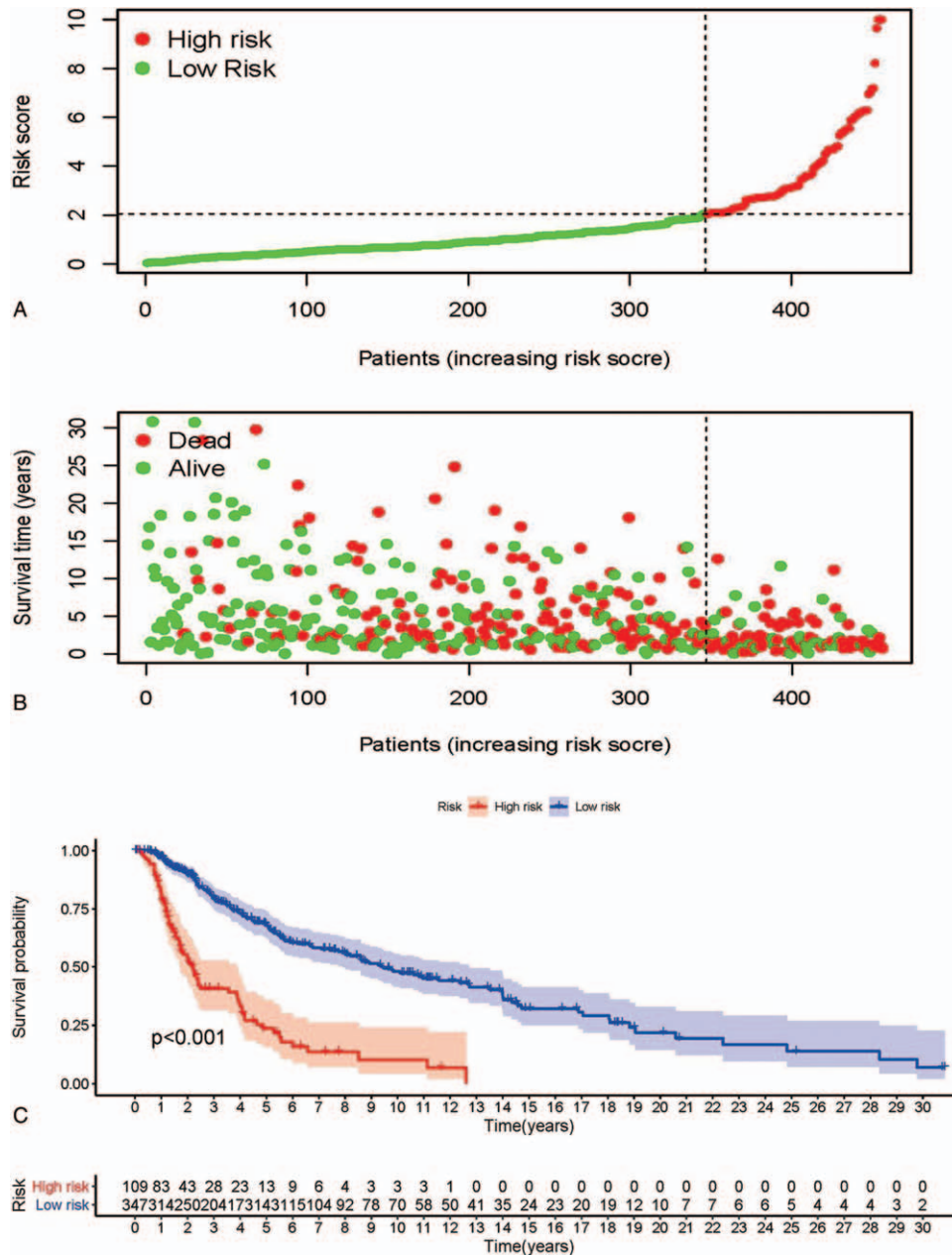


**Figure 5.** Clinical evaluation using the risk assessment model. (A) Risk scores and (B) survival outcomes for each case, and (C) K–M analysis.

conclusion in a retrospective study; they found that the prognosis of melanoma patients became worse with increasing age, reflecting the more aggressive tumor biology in older patients.<sup>[59]</sup> However, in contrast to Balch et al, we established a prognostic model of DEirlncRNA pairs, starting from irlncRNAs, to more deeply understand the level of immune regulation in patients in different risk groups. We also we used a more convenient way to build DEirlncRNA pairs, enabling us to judge the prognosis of patients without knowing their precise lncRNA expression levels.

However, the study had some limitations. First, the data were obtained from several public databases, and the clinical information downloaded from these databases was limited and incomplete. For example, we could only analyze and the IC<sub>50</sub> values of imatinib, paclitaxel, and cisplatin between the risk

model; there was a lack of sensitivity analysis for PD-1 and CTLA-4 inhibitors such as nivolumab and ipilimumab.<sup>[53]</sup> Second, with respect to signature preparation, we adopted a more efficient combination strategy. We determined specific transcription levels of DEirlncRNAs in the form of DEirlncRNA pairs; however, the conversion from a pair of expression levels to a 0 or 1 matrix entry is a one-way process. Finally, irlncRNAs are immune-related regulatory factors in the development of melanoma, and their molecular mechanisms need to be further studied to promote their potential clinical applications.

Overall, in this study, we identified a novel signature composed of irlncRNAs that does not require precise measurement of lncRNA expression levels to predict prognosis in melanoma patients. This signature may help to distinguish which patients are more likely to benefit from anti-tumor immunotherapy.

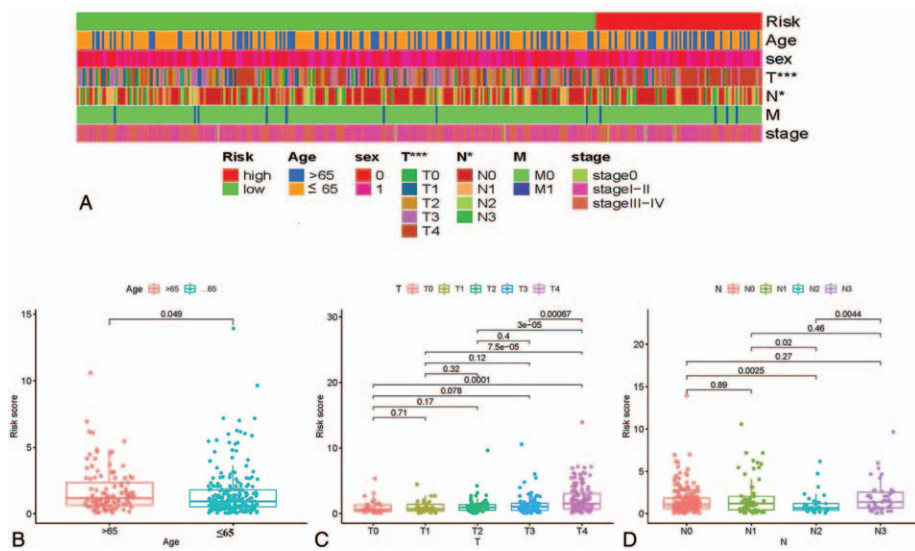


**Figure 6.** Clinical evaluation using the risk assessment model. (A) Strip chart and scatter diagram showing that age (B), T stage (C), and N stage (D) were significantly associated with risk score.

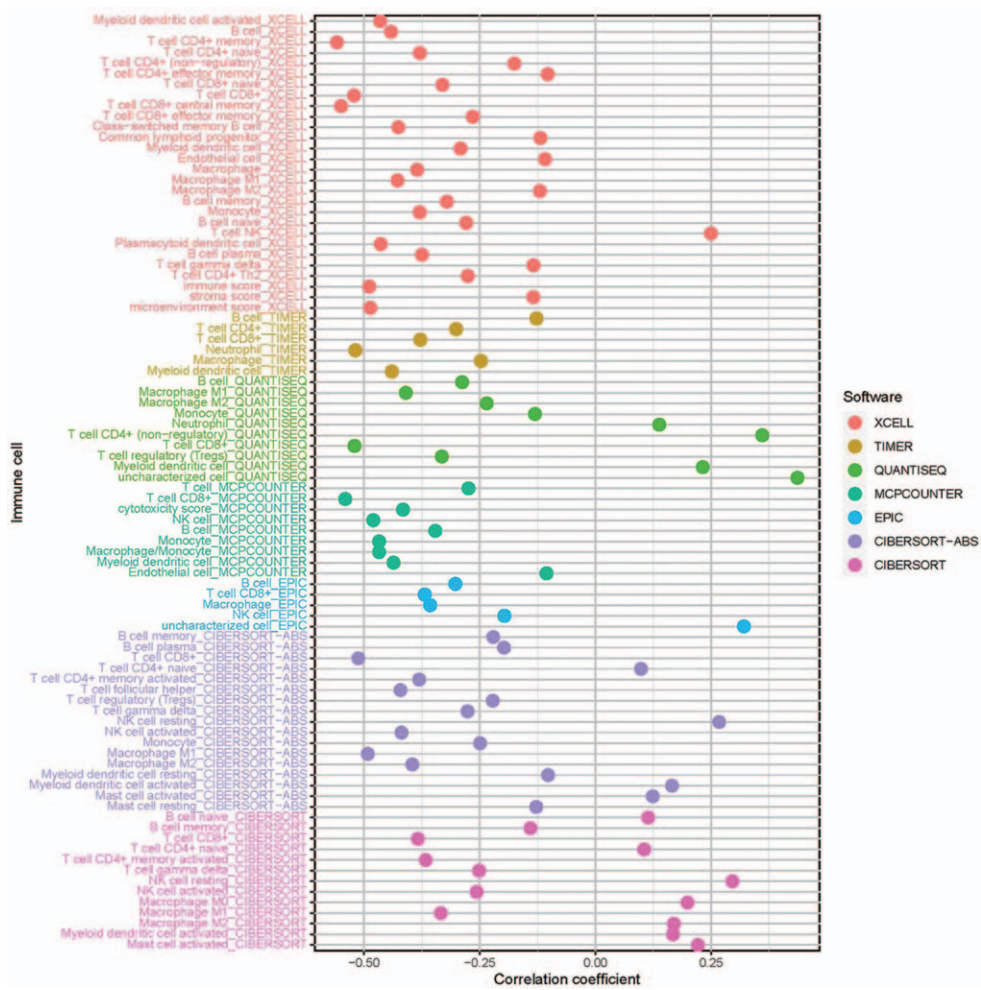


**Figure 7.** Estimation of tumor-infiltrating cells. Estimation of tumor-infiltrating cells by the risk assessment model. Patients in the high-risk group were more positively correlated with the infiltration of certain immune cells, including resting natural killer (NK) cells (CIBERSORT-ABS) and NK T cells (xCell). By contrast, they were negatively associated with CD4+ memory T cells (xCell) and CD8+ central memory T cells (xCell), etc.



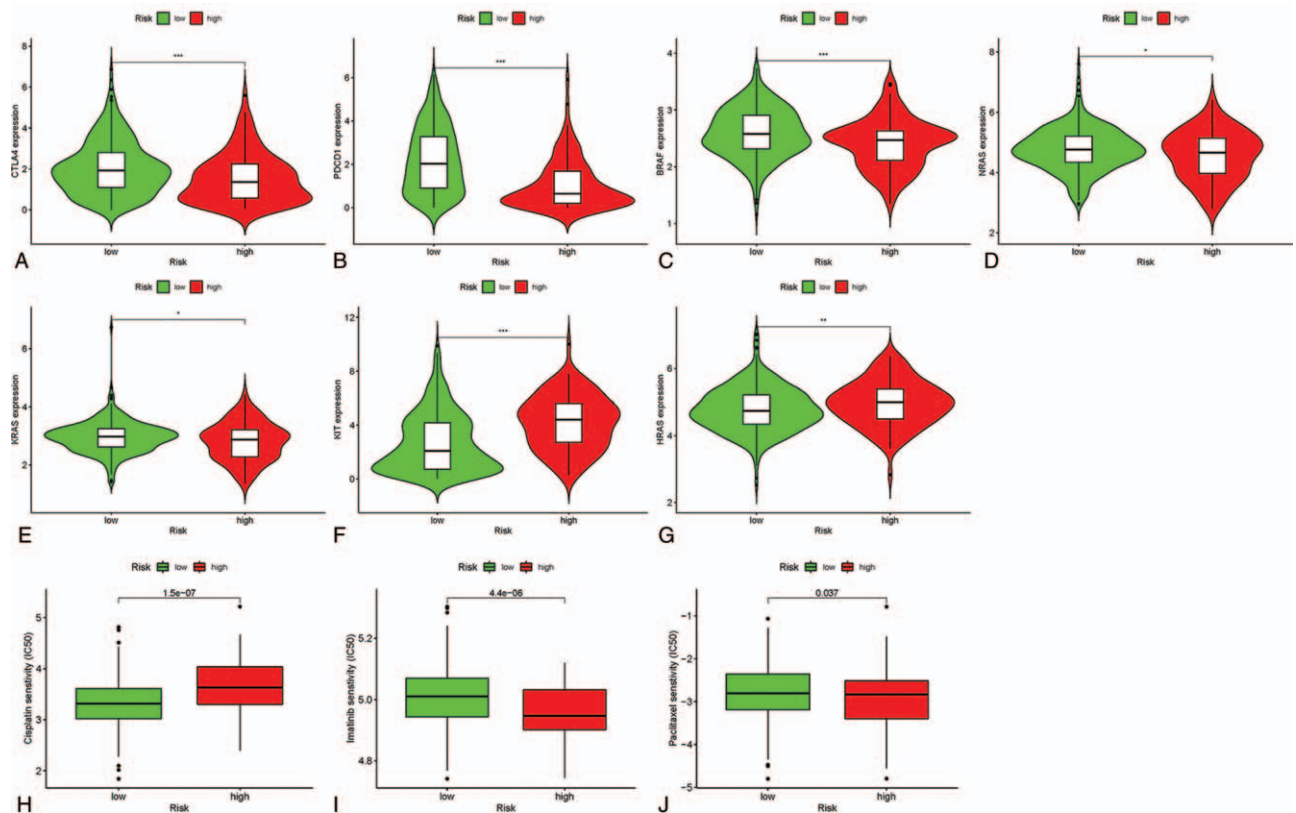


**Figure 8.** Estimation of ICI-related immunosuppressive molecules and kinase inhibitor molecules using the risk assessment model. High risk scores were positively correlated with downregulation of CTLA4 (A), PDCD1 (B), BRAF (C), NRAS (D), and KRAS (E), and with upregulation of KIT (F) and HRAS (G). The model is a potential predictor for chemosensitivity as high-risk scores were related to higher IC<sub>50</sub> values for cisplatin (H) and lower IC<sub>50</sub> values for imatinib (I) and paclitaxel (J).

## Acknowledgments

We are very grateful for the contributions of TCGA and GTEx database that provide information on cancer research, as well as all colleagues involved in the study.

## Author contributions

**Conceptualization:** Yu Jin.

**Data curation:** Zhehong Li, Junqiang Wei, Honghong Zheng, Yu Jin.

**Formal analysis:** Zhehong Li, Junqiang Wei, Yafang Zhang.

**Investigation:** Honghong Zheng, Mingze Song, Yafang Zhang.

**Methodology:** Zhehong Li, Honghong Zheng, Xintian Gan.

**Resources:** Zhehong Li, Mingze Song.

**Supervision:** Junqiang Wei.

**Validation:** Zhehong Li, Xintian Gan, Mingze Song, Yafang Zhang, Yu Jin.

**Visualization:** Zhehong Li, Junqiang Wei.

**Writing – original draft:** Zhehong Li, Junqiang Wei, Honghong Zheng.

**Writing – review & editing:** Junqiang Wei, Yu Jin.

## References

- [1] Siegel RL, Miller KD, Jemal A. Cancer statistics, 2019. *CA Cancer J Clin* 2019;69:7–34.
- [2] Bray F, Ferlay J, Soerjomataram I, et al. Global cancer statistics 2018: GLOBOCAN estimates of incidence and mortality worldwide for 36 cancers in 185 countries. *CA Cancer J Clin* 2018;68:394–424.
- [3] Ferlay J, Soerjomataram I, Dikshit R, et al. Cancer incidence and mortality worldwide: sources, methods and major patterns in GLOBOCAN 2012. *Int J Cancer* 2015;136:E359–86.
- [4] Wu XC, Eide MJ, King J, et al. Racial and ethnic variations in incidence and survival of cutaneous melanoma in the United States, 1999–2006. *J Am Acad Dermatol* 2011;65:S26–37.
- [5] Luke JJ, Flaherty KT, Ribas A, et al. Targeted agents and immunotherapies: optimizing outcomes in melanoma. *Nat Rev Clin Oncol* 2017;14:463–82.
- [6] Franklin C, Livingstone E, Roesch A, et al. Immunotherapy in melanoma: recent advances and future directions. *Eur J Surg Oncol* 2017;43:604–11.
- [7] Robert C, Long GV, Brady B, et al. Nivolumab in previously untreated melanoma without BRAF mutation. *N Engl J Med* 2015;372:320–30.
- [8] Wang LX, Wan C, Dong ZB, et al. Integrative analysis of long noncoding RNA (lncRNA), microRNA (miRNA) and mRNA expression and construction of a competing endogenous RNA (ceRNA) network in metastatic melanoma. *Med Sci Monit* 2019;25:2896–907.
- [9] Wang Y, Li J, Shao C, Tang X, et al. Systematic profiling of diagnostic and prognostic value of autophagy-related genes for sarcoma patients. *BMC Cancer* 2021;21:58doi: 10.1186/s12885-020-07596-5.
- [10] Han W, Hu C, Fan ZJ, et al. Transcript levels of keratin 1/5/6/14/15/16/17 as potential prognostic indicators in melanoma patients. *Sci Rep* 2021;11:1023doi: 10.1038/s41598-020-80336-8.
- [11] Lv Y, Lin SY, Hu FF, et al. Landscape of cancer diagnostic biomarkers from specifically expressed genes. *Brief Bioinform* 2020;21:2175–84.
- [12] Wilusz JE, Sunwoo H, Spector DL. Long noncoding RNAs: functional surprises from the RNA world. *Genes Dev* 2009;23:1494–504.
- [13] Hauptman N, Glavač D. Long non-coding RNA in cancer. *Int J Mol Sci* 2013;14:4655–69.
- [14] Peng W, Wang Z, Fan H. LncRNA NEAT1 impacts cell proliferation and apoptosis of colorectal cancer via regulation of Akt signaling. *Pathol Oncol Res* 2017;23:651–6.

- [15] Sun M, Liu XH, Wang KM, et al. Downregulation of BRAF activated non-coding RNA is associated with poor prognosis for non-small cell lung cancer and promotes metastasis by affecting epithelial-mesenchymal transition. *Mol Cancer* 2014;13:68doi: 10.1186/1476-4598-13-68.
- [16] Arun G, Diermeier S, Akerman M, et al. Differentiation of mammary tumors and reduction in metastasis upon Malat1 lncRNA loss. *Genes Dev* 2016;30:34–51.
- [17] Atianand MK, Caffrey DR, Fitzgerald KA. Immunobiology of long noncoding RNAs. *Annu Rev Immunol* 2017;35:177–98.
- [18] Li M, Liang M, Lan T, et al. Four immune-related long non-coding RNAs for prognosis prediction in patients with hepatocellular carcinoma. *Front Mol Biosci* 2020;7:566491doi: 10.3389/fmolb.2020.566491.
- [19] Wu Y, Zhang L, He S, et al. Identification of immune-related lncRNA for predicting prognosis and immunotherapeutic response in bladder cancer. *Aging* 2020;12:23306–25.
- [20] Liu Y, Gou X, Wei Z, et al. Bioinformatics profiling integrating a four immune-related long non-coding RNAs signature as a prognostic model for papillary renal cell carcinoma. *Aging* 2020;12:15359–73.
- [21] Fu Y, Yang J, Fan S, et al. A novel strategy facilitates reference gene selection by RT-qPCR analysis in kidney yang deficiency syndrome mice infected with the influenza A (H1N1) virus. *Biomed Res Int* 2020;2020:9075165doi: 10.1155/2020/9075165.
- [22] Cheung-Lee WL, Link AJ. Genome mining for lasso peptides: past, present, and future. *J Ind Microbiol Biotechnol* 2019;46:1371–9.
- [23] Augustyński J, Lenart J, Lipka G, et al. Reference Gene Validation via RT-qPCR for Human iPSC-Derived Neural Stem Cells and Neural Progenitors. *Mol Neurobiol* 2019;56:6820–32.
- [24] Guo X, Zhang B, Zeng W, et al. G3viz: an R package to interactively visualize genetic mutation data using a lollipop-diagram. *Bioinformatics* 2020;36:928–9.
- [25] Li T, Fan J, Wang B, et al. TIMER: a web server for comprehensive analysis of tumor-infiltrating immune cells. *Cancer Res* 2017;77:e108–10.
- [26] Newman AM, Liu CL, Green MR, et al. Robust enumeration of cell subsets from tissue expression profiles. *Nat Methods* 2015;12:453–7.
- [27] Aran D, Hu Z, Butte AJ. xCell: digitally portraying the tissue cellular heterogeneity landscape. *Genome Biol* 2017;18:220doi: 10.1186/s13059-017-1349-1.
- [28] Finotello F, Mayer C, Plattner C, et al. Molecular and pharmacological modulators of the tumor immune contexture revealed by deconvolution of RNA-seq data. *Genome Med* 2019;11:34doi: 10.1186/s13073-019-0638-6. Erratum in: *Genome Med* (2019) 11(1):50.
- [29] Becht E, Giraldo NA, Lacroix L, et al. Estimating the population abundance of tissue-infiltrating immune and stromal cell populations using gene expression. *Genome Biol* 2016;17:218doi: 10.1186/s13059-016-1070-5. Erratum in: *Genome Biol* (2016) 17(1):249.
- [30] Nelson ADL, Haug-Baltzell AK, Davey S, et al. EPIC-CoGe: managing and analyzing genomic data. *Bioinformatics* 2018;34:2651–3.
- [31] Newman AM, Steen CB, Liu CL, et al. Determining cell type abundance and expression from bulk tissues with digital cytometry. *Nat Biotechnol* 2019;37:773–82.
- [32] Carvajal RD, Antonescu CR, Wolchok JD, et al. KIT as a therapeutic target in metastatic melanoma. *JAMA* 2011;305:2327–34.
- [33] Agudo-López A, Prieto-García E, Alemán J, Pérez C, et al. Mechanistic added value of a trans-sulfonamide-platinum-complex in human melanoma cell lines and synergism with cis-platin. *Mol Cancer* 2017;16:45doi: 10.1186/s12943-017-0618-7.
- [34] Yan X, Sheng X, Chi Z, et al. Randomized phase II study of bevacizumab in combination with carboplatin plus paclitaxel in patients with previously untreated advanced mucosal melanoma. *J Clin Oncol* 2021;39:881–9.
- [35] Saranga-Perry V, Ambe C, Zager JS, et al. Recent developments in the medical and surgical treatment of melanoma. *CA Cancer J Clin* 2014;64:171–85.
- [36] Miller AJ, Mihm MC. Melanoma. *N Engl J Med* 2006;355:51–65.
- [37] O'Donnell JS, Teng MWL, Smyth MJ. Cancer immunoeediting and resistance to T cell-based immunotherapy. *Nat Rev Clin Oncol* 2019;16:151–67.
- [38] Huang D, Chen J, Yang L, et al. NKILA lncRNA promotes tumor immune evasion by sensitizing T cells to activation-induced cell death. *Nat Immunol* 2018;19:1112–25.
- [39] Sun Z, Jing C, Xiao C, et al. Long non-coding RNA profile study identifies an immune-related lncRNA prognostic signature for kidney renal clear cell carcinoma. *Front Oncol* 2020;10:1430doi: 10.3389/fonc.2020.01430.
- [40] Bruni D, Angell HK, Galon J. The immune contexture and immunoscore in cancer prognosis and therapeutic efficacy. *Nat Rev Cancer* 2020;20:662–80.
- [41] Hur K, Kim SH, Kim JM. Potential implications of long noncoding RNAs in autoimmune diseases. *Immune Netw* 2019;19:e4doi: 10.4110/in.2019.19.e4.
- [42] Zhang Y, Cao X. Long noncoding RNAs in innate immunity. *Cell Mol Immunol* 2016;13:138–47.
- [43] Guo L, Yao L, Jiang Y. A novel integrative approach to identify lncRNAs associated with the survival of melanoma patients. *Gene* 2016;585:216–20.
- [44] Zhang J, Liu H, Zhang W, et al. Identification of lncRNA-mRNA regulatory module to explore the pathogenesis and prognosis of melanoma. *Front Cell Dev Biol* 2020;8:615671doi: 10.3389/fcell.2020.615671.
- [45] Larkin J, Chiarion-Sileni V, Gonzalez R, et al. Combined nivolumab and ipilimumab or monotherapy in untreated melanoma. *N Engl J Med* 2015;373:23–34.
- [46] Helleday T, Eshtad S, Nik-Zainal S. Mechanisms underlying mutational signatures in human cancers. *Nat Rev Genet* 2014;15:585–98.
- [47] Zheng P, Zhou Z. Human Cancer Immunotherapy with PD-1/PD-L1 Blockade. *Biomark Cancer* 2015;7:15–8.
- [48] Topalian SL, Hodi FS, Brahmer JR, et al. Safety, activity, and immune correlates of anti-PD-1 antibody in cancer. *N Engl J Med* 2012;366:2443–54.
- [49] Shang J, Song Q, Yang Z, et al. Analysis of PD-1 related immune transcriptional profile in different cancer types. *Cancer Cell Int* 2018;18:218doi: 10.1186/s12935-018-0712-y.
- [50] Higashikawa K, Yagi K, Watanabe K, et al. <sup>64</sup>Cu-DOTA-anti-CTLA-4 mAb enabled PET visualization of CTLA-4 on the T-cell infiltrating tumor tissues. *PLoS One* 2014;9:e109866doi: 10.1371/journal.pone.0109866.
- [51] Ciszak L, Frydecka I, Wolowiec D, et al. Patients with chronic lymphocytic leukaemia (CLL) differ in the pattern of CTLA-4 expression on CLL cells: the possible implications for immunotherapy with CTLA-4 blocking antibody. *Tumour Biol* 2016;37:4143–57.
- [52] Burotto M, Chiou VL, Lee JM, et al. The MAPK pathway across different malignancies: a new perspective. *Cancer* 2014;120:3446–56.
- [53] Dhillon AS, Hagan S, Rath O, et al. MAP kinase signalling pathways in cancer. *Oncogene* 2007;26:3279–90.
- [54] Huang L, Chen H, Xu Y, et al. Correlation of tumor-infiltrating immune cells of melanoma with overall survival by immunogenomic analysis. *Cancer Med* 2020;9:8444–56.
- [55] Schupp J, Christians A, Zimmer N, et al. In-depth immune-oncology studies of the tumor microenvironment in a humanized melanoma mouse model. *Int J Mol Sci* 2021;22:1011doi: 10.3390/ijms22031011.
- [56] Ma XB, Xu YY, Zhu MX, et al. Prognostic signatures based on thirteen immune-related genes in colorectal cancer. *Front Oncol* 2021;10:591739doi: 10.3389/fonc.2020.591739.
- [57] Kümpers C, Jokic M, Haase O, et al. Immune cell infiltration of the primary tumor, not PD-L1 status, is associated with improved response to checkpoint inhibition in metastatic melanoma. *Front Med* 2019;6:27doi: 10.3389/fmed.2019.00027.
- [58] Mauldin IS, Wang E, Deacon DH, et al. TLR2/6 agonists and interferon-gamma induce human melanoma cells to produce CXCL10. *Int J Cancer* 2015;137:1386–96.
- [59] Balch CM, Soong SJ, Gershenwald JE, et al. Age as a prognostic factor in patients with localized melanoma and regional metastases. *Ann Surg Oncol* 2013;20:3961–8.